Dynamic Strategic Bond Analysis Yields a Ten-Step Synthesis of 20-nor-Salvinorin A, a Potent κ-OR Agonist

Jeremy J. Roach,[†] Yusuke Sasano,[†,#] Cullen L. Schmid,[‡] Saheem Zaidi,[§] Vsevolod Katritch,[§] Raymond C. Stevens,[§] Laura M. Bohn,[‡] and Ryan A. Shenvi*,[†]

[†]Department of Chemistry, The Scripps Research Institute, La Jolla, California 92037, United States

[‡]Departments of Molecular Therapeutics and Neuroscience, The Scripps Research Institute, Jupiter, Florida 33458, United States

[§]Departments of Chemistry and Biological Sciences, Bridge Institute, University of Southern California, Los Angeles, California 90089, United States

Ⓢ Supporting Information

ABSTRACT: Salvinorin A (SalA) is a plant metabolite that agonizes the human *kappa*-opioid receptor (κ-OR) with high affinity and high selectivity over *mu*- and *delta*-opioid receptors. Its therapeutic potential has stimulated extensive semisynthetic studies and total synthesis campaigns. However, structural modification of SalA has been complicated by its instability, and efficient total synthesis has been frustrated by its dense, complex architecture. Treatment of strategic bonds in SalA as dynamic and dependent on structural perturbation enabled the identification of an efficient retrosynthetic pathway. Here we show that deletion of C20 simultaneously stabilizes the SalA skeleton, simplifies its synthesis, and retains its high affinity and selectivity for the κ-OR. The resulting 10-step synthesis now opens the SalA scaffold to deep-seated property modification. Finally, we describe a workflow to identify structural changes that retain molecular complexity, but reduce synthetic complexity—two related, but independent ways of looking at complexity.

Structural complexity and synthetic complexity are related but not identical. Can they be productively decoupled?
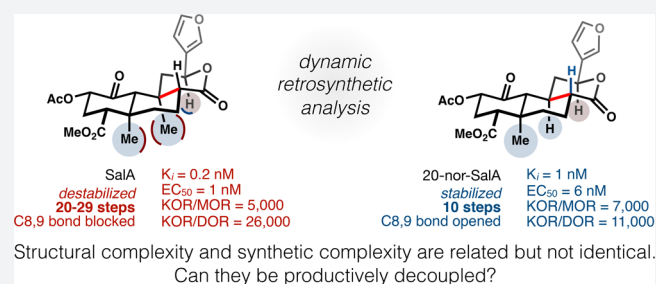
Drug overdose has become the leading cause of death for Americans under 50, driven largely by abuse of opioids.[1] The number of opioid-related deaths in 2015 surpassed 33 000,[2] which rivaled U.S. motor vehicle fatalities (35 000);[3] preliminary estimates from 2016 showed the annual rate continuing to rise.[4] To counter this epidemic, replacement of abused opioids with alternate pain therapeutics has emerged as an increasingly sensible goal.[5] One alternative anti-nociceptive target under investigation is the *kappa*-opioid receptor (κ-OR), a G protein-coupled receptor (GPCR) that is expressed throughout the nervous system and modulates consciousness, cognition, mood, and pain.[6,7] κ-OR-targeted analgesic development has focused on chemical property modification to generate peripherally restricted κ-OR agonists that lack central nervous system (CNS)-associated effects (e.g., hallucination),[8,9] or that promote biased signaling to minimize βarrestin-associated effects (e.g., sedation, dysphoria).[10] Among the more potent and selective agonists of the κ-OR is the brain-penetrant plant metabolite salvinorin A (SalA, **1**), which was identified as the primary psychoactive principle of *Salvia divinorum* and the most potent naturally occurring hallucinogen ever discovered.[11] As a result, SalA has been subject to semisynthetic modification[12,13] and total synthesis[14−17] to adjust its chemical properties and/or promote biased signaling of the κ-OR. Notably, a thiocyanate analogue of SalA, RB-64, was shown to strongly bias toward G protein-coupled signaling.[18] While many semisynthetic analogues of SalA have
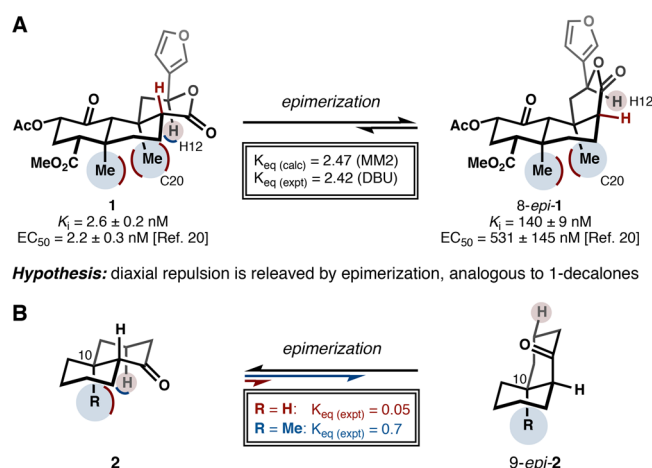
been explored, the most prolific investigators recently noted that its "chemical liabilities...narrow the available pool of viable chemical transformations."[13]

For example, both semisynthesis and total synthesis encounter the configurational lability of the C8 carbon, which undergoes epimerization to a lower affinity isomer, 8-*epi*-SalA (154−356-fold loss in potency).[19] The reaction mechanism has been hypothesized to involve either ring-fragmentation/reclosure or simple enolization/reprotonation, with the bulk of evidence pointing to the latter.[20] However, the driving force for this *trans*- to *cis*-ring fusion has not been identified. We believed a combination of lactone planarity and C20 axial-strain to be responsible (Figure 1). Analogy can be drawn to bridgehead (C10) methyl substitution of 1-decalone, which alters its *trans:cis* equilibrium ratio from 95:5 (C10−H) to 59:41 (C10-Me), driven by relief of the Me−C3−Hax 1,3-diaxial interaction in the *cis*-isomer.[21] In order to stabilize the scaffold and attenuate epimerization, C20 of SalA might be resected through chemical synthesis, whereas semisynthetic removal would be difficult. The effect of this modification on the chemical synthesis itself is profound.

When strategic bonds (SBs)[22,23] in SalA are considered, the quaternary carbon (C9) bearing the C20 methyl reveals its

Figure 1. Chemical instability of SalA. (A) Calculation predicts and experimentation has shown that SalA is disfavored to 8-epi-SalA approximately 2.5:1. This epimerization leads to significant loss in potency. (B) We hypothesized that the driving force for this epimerization is partly diaxial repulsion between C20 and H12, which is relieved in the *cis*-fused isomer, analogous to 10-methyl-1-decalone epimerization. Therefore, like 1-decalone, C20 (methyl) deletion should stabilize the SalA scaffold.

importance. Two SBs in SalA take priority over other possibilities through the large reduction of complexity associated with their cleavage: a C12−O lactonization transform removes a heteroatom bond, ring, and stereocenter, and a C8−9 Michael transform removes a ring and three stereocenters, leaving a simple cyclohexanone. However, strategic prioritization of the C9−10 bond ignores stereocontrol, which suffers from the small potential energy calculated to separate subtargets **i−iii** from stereoisomers **iv−vi** (Figure 2). As a result of the diaxial C19/C20 methyls, **i** and **iii** only favor the desired *trans*-decalone by a slim margin, and alkyne **ii** heavily favors the *cis*-decalone **v**. Notably, the four prior total syntheses avoid decalone intermediates altogether, despite their simplicity. Furthermore, precursor **3** contains a tetrasubstituted neopentyl alkene (C9=10) in which one substituent is a quaternary carbon, which is difficult to form due to A^{1,3} strain.

These problems abate if the target is treated not as static but as dynamic. The C9−10 bond becomes strategic for disconnection only by resection of the C20 methyl; C9−10 can be considered a "dynamic strategic bond." Three benefits emerge. First, the intermediate *trans*-decalin (**vii**) is calculated to predominate over the *cis*-isomer (**viii**), in contrast to **i−iii** vs **iv−vi** (Figure 3). Second, the unsaturated cyclohexanone precursor would arise from condensation of a β,β-disubstituted cyclohexenolate with an aldehyde instead of a methyl ketone: the latter is a challenging reaction for which we found no precedent. Third, 20-nor-SalA is calculated to be more stable than its C8-epimer, reversing the configurational preferences of SalA itself. Taken together, there is only one reason not to resect C20: 20-nor-SalA is an unknown molecule with unknown binding affinity to the κ-OR.

The prospect of undertaking a total synthesis of a complex molecule for application opioid receptor pharmacology with no guaranteed target affinity was daunting. So, we first explored the binding of 20-nor-SalA to the κ-OR *in silico*. However, the recent crystal structure of a κ-OR with antagonist JDTic[6] reflects an inactive state conformation of the binding pocket, specific to JDTic, and therefore is not well suited for binding of
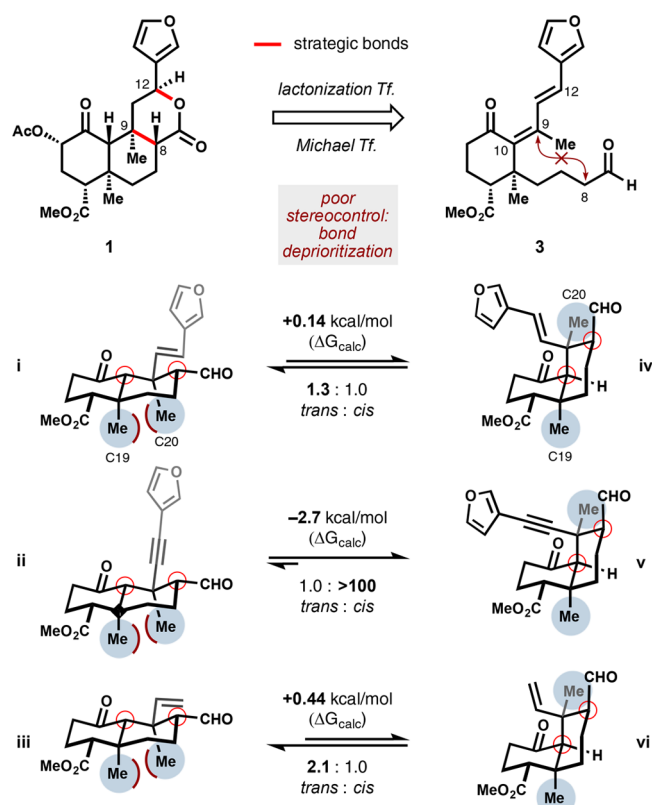

Figure 2. Retrosynthetic analysis of **1** using strategic bond analysis. In addition to SalA scaffold destabilization, C20 destabilizes intermediate decalones and thus deprioritizes a key strategic bond (C8−9). C20 also frustrates precursor (**3**) synthesis as a substituent on a *tert*-alkyl tetrasubstituted alkene.
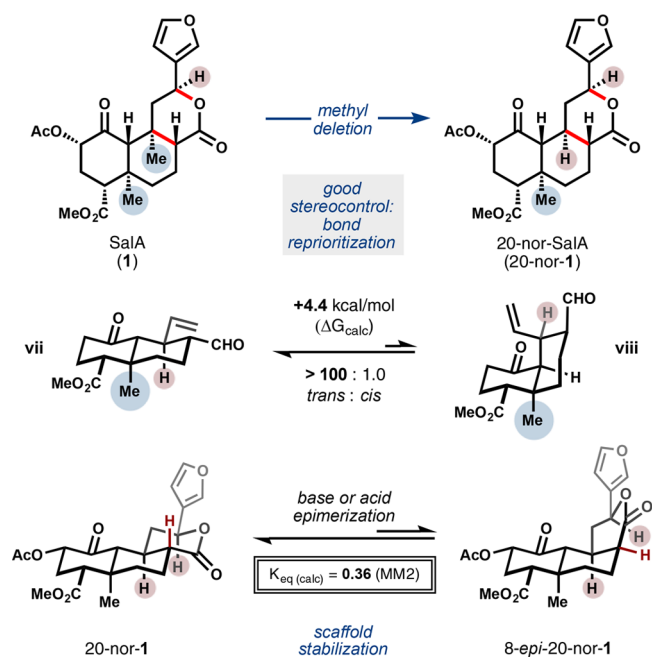
Figure 3. Effect of C20 deletion on scaffold stability. Treatment of SalA as a dynamic structure unlocks the C9−10 strategic bond (SB) for Michael transform by C20 deletion. Both decalone intermediates and the SalA scaffold itself are stabilized. The Michael reaction precursor (shown in Figure 5) becomes very easy to synthesize.

agonist SalA or its analogues. Therefore, we developed an active-like model of the κ-OR by using homology modeling based on an active state agonist-bound crystal structure of the mu-opioid receptor (μ-OR) (PDB ID: 5c1m). Receptor modeling included thorough sampling and optimization of the binding pocket side chains. The resulting active-like κ-OR receptor model was used to dock SalA and 20-nor-SalA using an all-atom global energy optimization algorithm, based on Monte Carlo sampling of the ligand and residue side chains within 4 Å of the ligand.[24] In the predicted docking models SalA and 20-nor-SalA bind in similar poses and with comparable binding scores (−28.76 and −27.42, respectively). In this binding pose 20-nor-SalA forms polar interactions with Q115[2.60], Y312[7.35], and C210[ECL2] residues and, potentially, with N122[ECL1] and/or R202[ECL2] residues. The ligands also make extensive hydrophobic interactions with residues lining transmembrane 2, 3, and 7 including V118[2.63], W124[ECL1], I135[3.29], and I316[7.39] residues. This pose also satisfies the ligand interaction contacts derived from mutagenesis data for SalA.[25] In this pose, the 20-methyl group is directed toward the extracellular region with no apparent interactions with the receptor. This binding pose suggested comparable binding affinity for SalA and its 20-nor derivative.
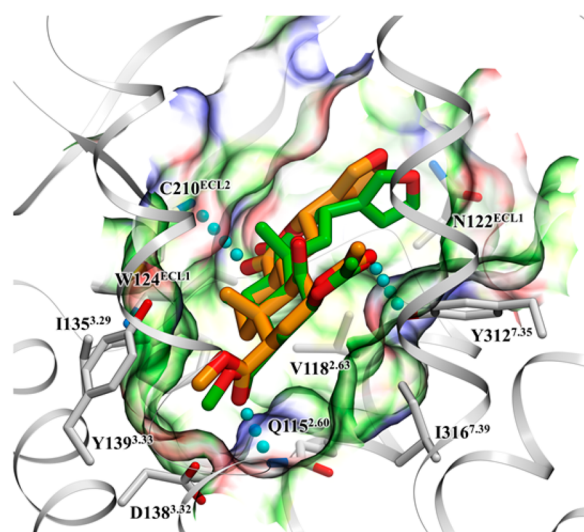
Figure 4. Calculated binding to the κ-OR. Docking mode of ligands 20-nor-SalA (orange) and SalA (green), shown in stick representations inside the kappa opioid receptor model (white colored cartoon representation). Residues in the ligand vicinity are shown in white-colored stick representation, and associated hydrogen bonds are shown in cyan colored dots.

These calculations provided a theoretical basis for investigation; justification for total synthesis usually depends on experimentally observed activity. However, knowledge of κ-OR affinity in this case required synthesis—a catch-22. A study to probe structure−activity relationships in SalA could not reach the nor-20 target,[26] so no empirical data was available. Nevertheless, we felt the potential benefits for therapeutic development outweighed the risk. Furthermore, the simplification imparted by C20 resection significantly improved material access by unlocking the C9−10 bond, whereas prior syntheses of SalA produced only small amounts of late-stage material over multiple operations (20−29 steps; 0.7−1% yield).[14−17] Shown in Figure 5 is a 10-step synthesis of 20-nor-SalA.

The synthesis commenced from Hagemann's ester (**4**), a commercially available building block common in terpene synthesis,[27] which appeared to be an obvious precursor to 20-nor-SalA via vicinal difunctionalization. Grignard reagent **5** was generated from commercially available *tert*-butyl(4-chlorobutoxy)dimethylsilane and used directly. However, early experiments to trap the sterically encumbered enolates resulting from conjugate addition proved fruitless, even with the simplest electrophiles like acetaldehyde. Enolate trans-metalation with diethylzinc allowed enol silane formation and Mukaiyama aldol addition,[28] but always in low yield and never with electron-rich aldehydes. Instead, we found that addition of zinc chloride[29,30] and five equivalents of acrolein resulted in efficient formation of **6** as an inconsequential 6:1 mixture of allylic alcohols. Elimination of this alcohol was effected by mesylation, followed by ketone enolization by addition of DBU. These conditions initially delivered a mixture of (*E*)- and (*Z*)-dieneones, but isomerization mediated by reversible DBU addition occurred with prolonged reaction time to favor (*E*)-**7** with 20:1 selectivity.

Subsequent steps for elaboration to 20-nor-**1** involved careful choreography of (1) cyclization, (2) α-acetoxylation, (3) aryl appendage, and (4) lactonization steps, based on extensive reconnaissance briefly discussed here. An initial Heck arylation of **7** with 3-bromofuran or its boronic esters proved low yielding, and δ-(3-furyl)-substitution lowered the electrophilicity of the dienone toward nucleophiles. Several ketone α-hydroxylations competitively oxidized the furan ring if present, and Hagiwara's conditions for acetate installation by Mitsunobu stereoinversion[15] were inefficient and required purification from 20 equiv of PPh$_3$ and 10 equiv of diisopropyl azodicarboxylate. The aldehyde, not carboxylic acid oxidation state, was chosen to engage in Michael addition due to its ease of enolization (or enamine formation) in the presence of the two other enolizable carbonyls. As a result, the final sequence involved *tert*-butyldimethylsilyl removal with 2 M HCl, followed by Swern oxidation of the deprotected alcohol to aldehyde **8**. Intramolecular Michael addition was carried out from the corresponding pyrrolidine enamine in methanol/tetrahydrofuran with added acetic acid. As the alcoholic cosolvent increased in size, the ratio of *trans*- and *cis*-decalone (see Figure 5B) increasingly favored the undesired *cis*-decalin. Quench by potassium carbonate served to equilibrate an initially low ratio of *trans-/cis*-decalones to predominantly one isomer **9** (*cis*-decalone lower than 5% content by crude ¹H NMR), which contained the contiguous stereopentad found in the salvinorin A scaffold. Substitution of methanol cosolvent with ethanol resulted in a dramatically slower equilibration. Pinnick oxidation of aldehyde **9** capped a facile route to diversifiable carboxylic acid (**10**, X-ray confirmation), which was successfully scaled to 5.3 g in a single pass. After much experimentation, we found only four steps to separate **10** from 20-nor-SalA, affording a convenient platform for eventual diversification to alter the chemical properties of the SalA chemotype.

The first two of these steps address appendage of the equatorial acetate, which is challenged by the high selectivity for axial approach of electrophiles,[16] the difficulty of S$_N$2 stereoinversion of these axial α-hydroxy and α-bromo cyclohexanones, and the high oxidation potential of furanyl intermediates. In some cases, α-debromination by acetate outcompeted substitution. These problems were solved by deprotonation of **10** with 2.1 equiv of LDA followed by Davis

A

B
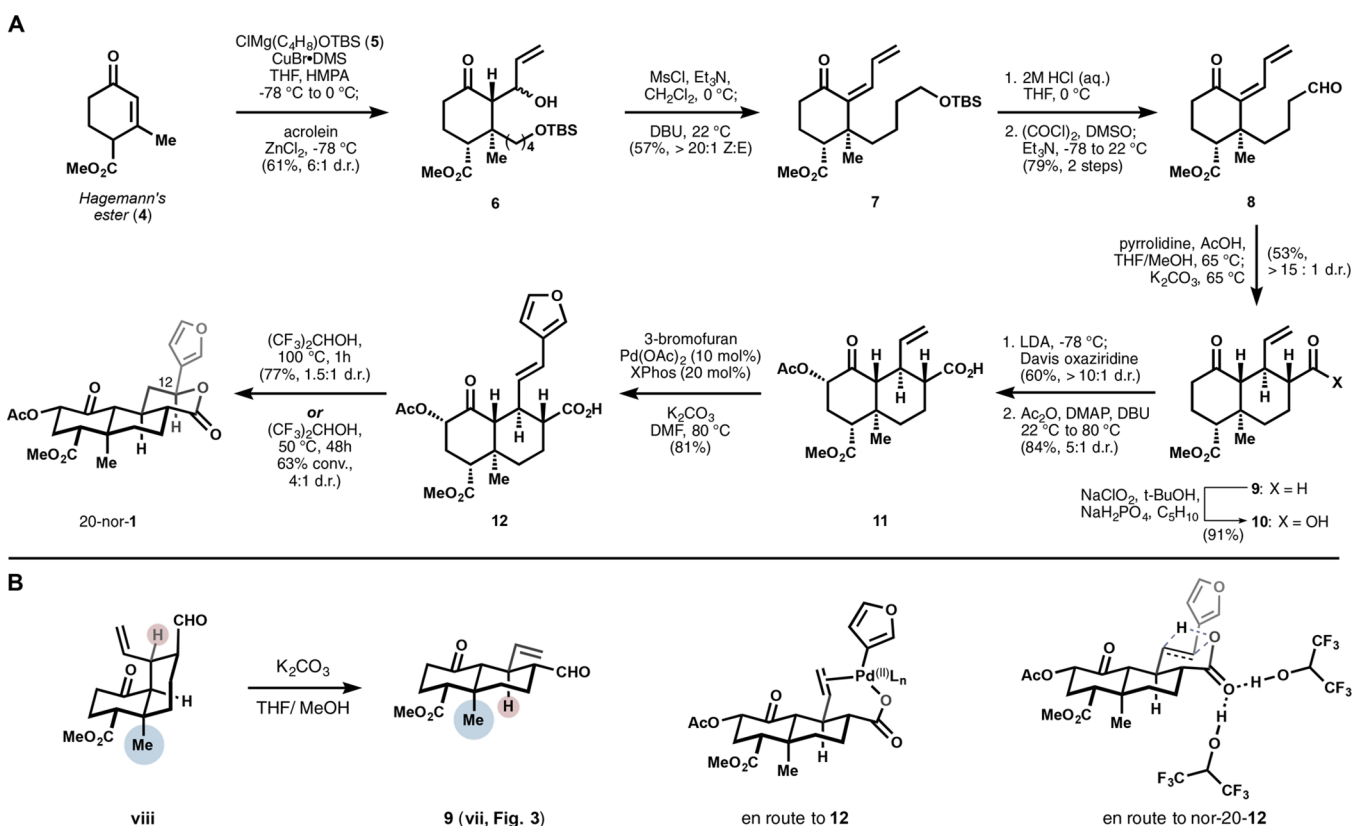

Figure 5. Chemical synthesis of 20-nor-salvinorin A. (A) Commercially available materials **4** and **5** are advanced in 10 steps to 20-nor-**1** via diversifiable scaffold **11**, which is accessed in 7% overall yield. (B) Confirmed and hypothesized intermediates in the Michael (**8** → **9**), Heck (**11** → **12**), and lactonization (**12** → 20-nor-**1**) steps. TBS, *tert*-butyldimethylsilyl; DMS, dimethylsulfide; THF, tetrahydrofuran; HMPA, hexamethylphosphoramide; MsCl, methanesulfonyl chloride; DBU, 1,8-diazabicyclo(5.4.0)undec-7-ene; DMSO, dimethyl sulfoxide; LDA, lithium diisopropylamide; DMAP,4-dimethylaminopyridine; XPhos, 2-dicyclohexylphosphino-2′,4′,6′-triisopropylbiphenyl; DMF, *N,N*-dimethylformamide.

oxaziridine[31] addition, which generated in high diastereoselectivity the axial α-hydroxy-decalone. Subsequent acetylization occurred at both the alcohol and the carboxylic acid; warming this reaction mixture led to equilibration to favor the equatorial acetate without affecting the stereochemistry at any other position. Careful aqueous workup was performed to decompose the mixed anhydride at high pH and recover the carboxylic acid at low pH, while sparing the acetate from cleavage during these operations.

The carboxylic acid itself was found to be crucial for the Heck arylation with 3-bromofuran. Early experiments to arylate the electronically unbiased olefin of aldehyde **9** surveyed a range of palladium sources, oxidants, ligands, solvents, and bases, under both oxidative[32] and traditional Heck conditions with little success. The optimal results in these early versions of the synthesis required 10 portion-wise additions of palladium-(II) acetate, 3-furanylboronic acid, and a bifluoride source. Ultimately, the yield, reproducibility, and enthusiasm for this intensive procedure were low. Fortunately, we discovered that carboxylic acids **10** or **11** (in contrast to aldehyde **9**) underwent very efficient Heck arylation as their alkali salts: the potassium carboxylate provided the highest yields of **12** and XPhos ligands promoted the highest rates and catalyst turnovers. The superiority of carboxylic acids to the corresponding aldehyde may derive from accelerated coordination/migratory insertion by initial coordination of the 3-furyl-palladium(II) by the potassium carboxylate (Figure 5B). Analogy can be drawn to classic proximity effects[33] recently brought to bear on palladium catalysis using carboxylic acids.[34] To the best of our knowledge,

the closest precedent in the Heck reaction of haloarenes[35] involves the accelerated arylation of unsaturated primary amides compared to their corresponding phthalimides.[36]

The final obstacle to 20-nor-**1** required lactonization of the carboxylic acid onto an electron-rich conjugated alkene with Markovnikov regioselectivity and equatorial stereoselectivity—on its face an uncomplicated scenario. We were dismayed to discover that subjection of **12** to a variety of strong Brønsted acids led to furan decomposition at rates competitive with lactonization, and what little lactones could be recovered were equimolar mixtures of diastereomers at C12. The same lactones were generated in trace quantities by the Heck reaction (**11** → **12**), possibly by a Pd–H-mediated pathway,[37] but never in preparatively useful yields, nor with stereoselectivity. Experimentation with radical-polar crossover cyclization[38] and Lewis acid-assisted cyclization honed in on Bi(OTf)$_3$ in hexafluoroisopropanol (HFIP) solvent as the highest yielding conditions that exhibited good lactonization rate (61%, $t_{1/2}$ = 30 min at 0 °C), but no stereoselectivity. We were surprised to find that HFIP solutions of **12** in the absence of any Lewis acids underwent lactonization, albeit with substantially decreased rates ($t_{1/2}$ = 3.5 days at 40 °C). These were the only conditions to exhibit stereochemical preference for 20-nor-**1** (4:1 d.r. @ 63% conversion). Neither trifluoroethanol (TFE, pK_a = 12.4)[39] nor nonafluoro-*tert*-butanol (pK_a = 5.2) promoted efficient lactonization, even at elevated temperature (90 °C), highlighting the idiosyncracy of HFIP (pK_a = 9.3). Weak and moderate Brønsted acids (CH$_3$CO$_2$H, pK_a = 4.8; phenol, pK_a = 10; CF$_3$CO$_2$H, pK_a = −0.25) did not cause any reaction at
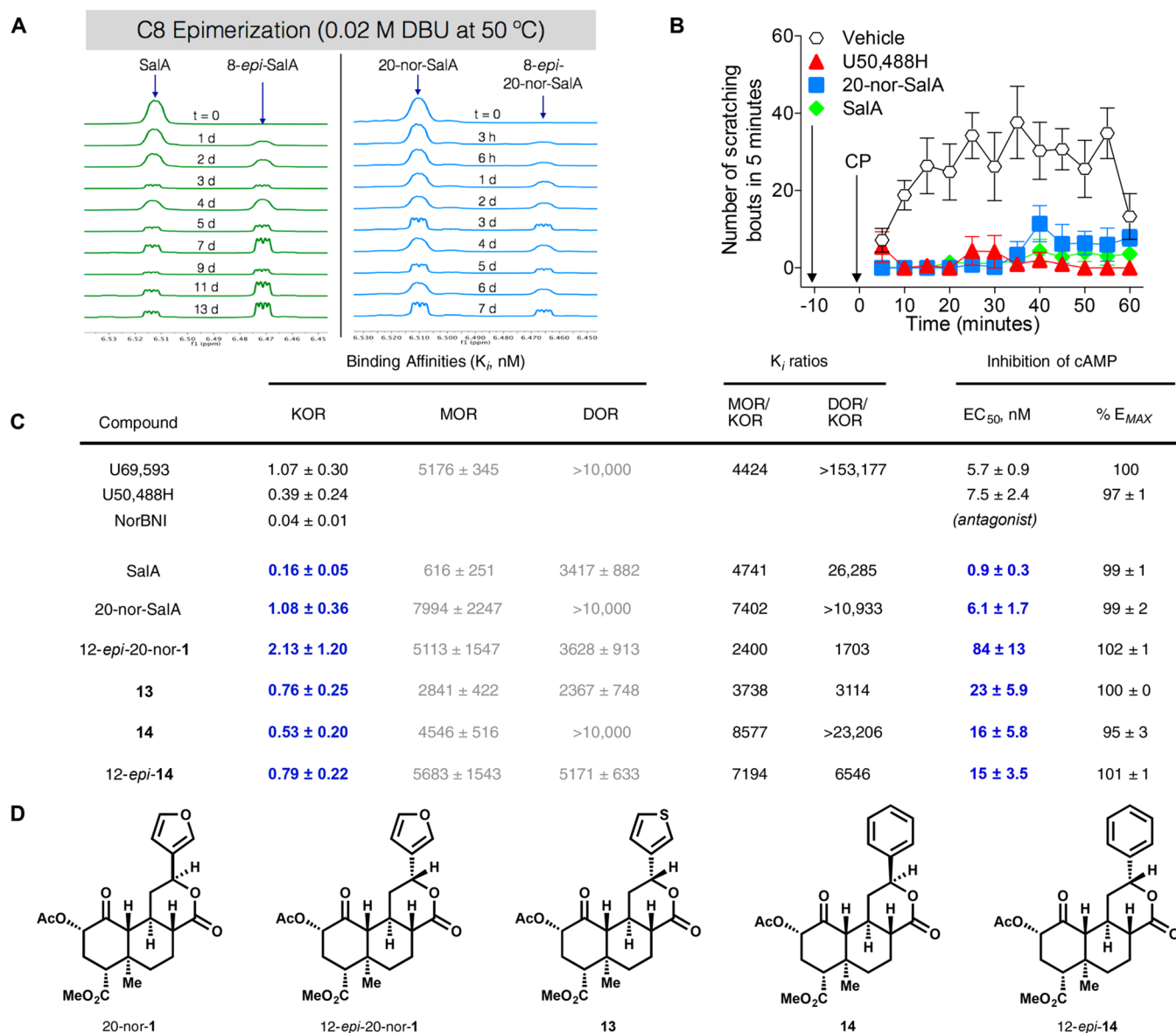
Figure 6. Comparison of chemical reactivity and biological activity of 1 and 20-nor-1. (A) Treatment of **1** and 20-nor-**1** with DBU in MeCN-d_3 at 50 °C results in slow epimerization at C8. However, **1** favors 8-*epi*-**1** (equilibrium after 11 days), whereas 20-nor-**1** is more stable than its C8 epimer (equilibrium after 3 days). (B) *Kappa* agonists suppress chloroquine phosphate-induced pruritus in mice.[10,40] Chloroquine phosphate (CP 40 mg/kg, s.c.) was administered 10 min following a 3 mg/kg, (s.c.) injection of each compound and scratching behaviors were monitored over time. All compounds suppressed the itch response at this dose over time compared to vehicle (1:1:8, DMSO:Tween 80:0.9% sterile saline) pretreatment (interaction of time and drug: $F_{(36, 273)}$ = 19.87, $p < 0.0001$, 2-way ANOVA (n = 10 veh, 5 U50, 5 20-nor-SalA, 5 SalA). (C) Affinity and functional signaling parameters at the human KOR expressed in CHO-K1 cells.[41,42] Radioligand competition binding assays were performed against 3H-U69,593 to determine K_i (n = 3−9). Competition binding with ^{3}H-DAMGO and ^{3}H-Diprenorphine was performed to determine affinity at μ-OR and δ-OR (n = 3). Inhibition of cAMP accumulation was used to determine EC50 and E_{MAX} values by nonlinear regression analysis (n = 6−8). Data are shown as the mean ± SEM. (D) Analogues synthesized from intermediate **11** using the same sequence as Figure 5.

room temperature, whereas strong Brønsted acids (CF₃SO₃H, pK_a = −14) caused nonstereoselective lactonization concomitant with decomposition. The lactonization is reversible in HFIP: at elevated temperatures 20-nor-**1** equilibrates to **12** and 12-*epi*-20-nor-**1** with no stereoselectivity but favoring the lactones. Therefore, the stereoselectivity imparted by HFIP is not thermodynamic but kinetically determined. All of these observations exclude an intermolecular alkene protonation by HFIP, and instead may derive from acidification of the substrate carboxylic acid via a hydrogen bonding network, followed by internal protonation and collapse of the ion pair (Figure 5B). For preparative purposes, we have found it easiest to generate

20-nor-**1** with high conversion from **12**, but with low stereoselectivity since 12-*epi*-20-nor-**1** is easily separable. Alternatively, we can halt these reactions at low conversion and good stereoselectivity (e.g., 63%, 4:1 d.r.), which may be useful for analogues whose diastereomers are inseparable.

Access to 20-nor-**1** allowed us to compare its chemical reactivity and biological activity to **1**. As reported by multiple investigators, SalA is undergoes epimerization under basic conditions to disfavor the natural configuration at C8. Similarly, we found 0.5 equiv of DBU in acetonitrile-d_3 generates a 29:71 mixture of **1**:8-epi-**1** at 50 °C (Figure 6A). In contrast, this relative stability is reversed in 20-nor-SalA: under identical

conditions the equilibrium holds at 70:30, close to the calculated K_{eq} (Figure 3). More importantly, 20-nor-SalA retains high affinity for the κ-OR, as measured by radioligand competition binding against [³H]-U69,593. It also behaves as a full agonist in G protein signaling assays measured by the inhibition of forskolin-stimulated, adenylyl cyclase-mediated, cAMP accumulation. The pharmacological properties of 20-nor-SalA closely match the conventional, selective agonist U69,593, although SalA has slightly higher affinity and efficacy than either (Figure 6C). While we consider our chemical synthesis to be more useful for scaffold diversification than for large-scale production, its brevity has allowed us to prepare enough material (>75 mg) to test its properties in vivo. κ-OR agonists suppress non-histamine-related itch in rodents and in humans, so we evaluated the ability of 20-nor-**1** to suppress itch in mice, and found it similarly effective to SalA and another conventional agonist (U50,488H) (Figure 6B) indicating a functional equivalence.

Preliminary proof-of-principle for the generality of this route, especially the late stage carboxylate-accelerated Heck reaction and alkene lactonization, was established by the synthesis of aryl analogues that have been inaccessible by semisynthetic modification of isolated **1** (Figure 6D). For example, a thiophene has never been substituted for the naturally occurring furan, as in **13**, which exhibits high binding affinity but reduced agonism compared to 20-nor-**1**. Similarly, purely unsubstituted phenyl analogues of 20-nor-**1** (**14**) retain the same binding affinity as their furyl counterparts, even the C12-epimer of **14**. This observation stands in contrast to prior analogues formed by cycloaddition of dimethylacetylene dicarboxylate with **1** whose disubstituted phenyl rings led to 31−39 fold losses in binding affinity.[43] None of our analogues show appreciable binding to the alternative μ- or δ-opioid receptors (μ-OR/ δ-OR), maintaining the high receptor selectivity of **1**. Thus, a small handful of analogues has already opened opportunities for scaffold alteration, and this information should aid the design of analogues with modified physical properties.[44]

As demonstrated here, the integration of structure perturbation, *in silico* docking, and retrosynthetic analysis can advance the use of complex secondary metabolites (natural products) as drug leads (Figure 7, visualized using the Rubik's Cube analogy, as in ref 45). The attributes of secondary metabolites have been embraced as useful library characteristics, especially high-fraction sp³ content, improving selectivity and hit rate.[46−48] These same attributes can lead to arduous synthesis campaigns and have prompted scaffold redesign to significantly reduce complexity.[49] While structural complexity and synthetic complexity are related, they are nonidentical: synthesis can be simplified while structural complexity is maintained.[49,50] We hope to apply the approach demonstrated manually here—computed affinity/dynamic retrosynthetic analysis—to minimally perturb complexity[51] and affinity, only enough to reveal the most efficient retrosynthetic path. A docking program coupled to traditional retrosynthesis search algorithms[23,45] might easily be deployed against complex metabolites with known targets. Although restricted to a single illustration, this approach has proved successful for the salvinorin chemotype of κ-OR agonist. By deletion of a single methyl group (C20), identified here as the primary driving force for C8 epimerization, we have simultaneously stabilized the salvinorin scaffold and simplified its synthesis, while maintaining target engagement.[52] This chemical platform
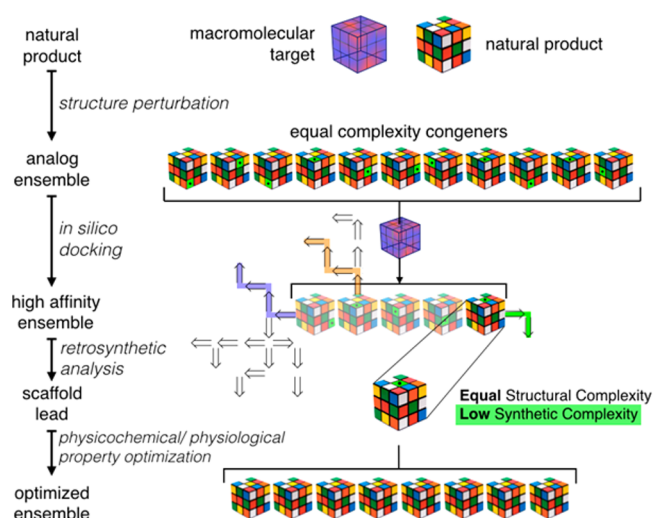
Figure 7. Workflow for computed affinity dynamic retrosynthesis. Iterative computation could accelerate deployment of complex metabolites as drug leads. First, random structural mutation of a complex scaffold would generate an ensemble of equally complex analogues. Second, *in silico* docking using a validated computational model would screen out poor binders and generate an enriched ensemble. Third, retrosynthesis search algorithms would identify scaffolds from among this enriched ensemble that maintain the high structural complexity of the natural product (secondary metabolite), but possess reduced synthetic complexity. A medicinal chemistry campaign would thus be accelerated by facile total synthesis, accelerating optimization of properties.

includes a carboxylate-directed Heck reaction and an unusual fluorous alcohol-promoted lactonization, which are capable of generating previously inaccessible analogues that retain high potency at the κ-OR and high selectivity against other opioid receptors. Additional modification of the 20-nor-SalA scaffold will focus on improvement of half-life in blood, bioavailability, peripheral nervous system restriction, and bias against βarrestin recruitment, as well as further scaffold stabilization. Success in these goals should deliver multiple candidates for next generation analgesics.

■ ASSOCIATED CONTENT

Ⓢ Supporting Information

The Supporting Information is available free of charge on the ACS Publications website at DOI: 10.1021/acscentsci.7b00488.

> NMR spectra, X-ray crystallographic data (PDF)
>
> Protein docking structures (PDB1, PDB2)
>
> Crystallographic data for **10** and 20-nor-**1** are available free of charge from the Cambridge Crystallographic Data Centre (CCDC) under reference numbers 1569390 and 1569389 (CIF1, CIF2)

■ AUTHOR INFORMATION

Corresponding Author

*E-mail: rshenvi@scripps.edu.

ORCID Ⓘ

Vsevolod Katritch: 0000-0003-3883-4505

Ryan A. Shenvi: 0000-0001-8353-6449

Present Address

#Graduate School of Pharmaceutical Sciences, Tohoku University, 6-3 Aoba, Aramaki, Aoba-ku, Sendai 980-8578, Japan.

Author Contributions

J.J.R. and Y.S. designed and performed synthetic experiments, and analyzed the corresponding data, with R.A.S. assisting. C.L.S. designed and performed biological assays, and analyzed the corresponding data. S.Z. and V.K. designed and performed docking experiments and analyzed the corresponding data. R.C.S., L.M.B., and R.A.S. supervised the project. R.A.S. wrote the manuscript.

Notes

The authors declare the following competing financial interest(s): A chemical process patent has been filed on the synthetic route, U.S. Patent Appl. 62,519,363.

■ REFERENCES

(1) Katz, J. Drug Deaths in America Are Rising Faster Than Ever. *New York Times*, 2017, https://www.nytimes.com/interactive/2017/06/05/upshot/opioid-epidemic-drug-overdose-deaths-are-rising-faster-than-ever.html.

(2) U.S. National Institute on Drug Abuse, Overdose Death Rates, 2017; https://www.drugabuse.gov/related-topics/trends-statistics/overdose-death-rates.

(3) National Highway Traffic Safety Administration's National Center for Statistics and Analysis, *2015 Motor Vehicle Crashes: Overview*, Report No. DOT HS 812 318, 2016; https://crashstats.nhtsa.dot.gov/Api/Public/ViewPublication/812318.

(4) Ahmad, F. B. Quarterly provisional estimates for selected indicators of mortality, 2015-Quarter 4, 2016. (National Center for Health Statistics, National Vital Statistics System, Vital Statistics Rapid Release Program, 2017).

(5) Skolnick, P.; Volkow, N. D. Re-energizing the development of pain therapeutics in light of the opioid epidemic. *Neuron* **2016**, *92*, 294−297.

(6) Wu, H.; et al. Structure of the human κ-opioid receptor in complex with JDTic. *Nature* **2012**, *485*, 327−334.

(7) Vanderah, T. W. Delta and kappa opioid receptors as suitable drug targets for pain. *Clin. J. Pain* **2010**, *26*, S10−S15.

(8) Stein, C. Targeting pain and inflammation by peripherally acting opioids. *Front. Pharmacol.* **2013**, *4*, 123−125.

(9) Vadivelu, N.; Mitra, S.; Hines, R. L. Peripheral opioid receptor agonists for analgesia: a comprehensive review. *J. Opioid Manag.* **2011**, *1*, 55−68.

(10) Brust, T. F.; et al. Biased agonists of the kappa opioid receptor suppress pain and itch without causing sedation or dysphoria. *Sci. Signaling* **2016**, *9*, ra117.

(11) Roth, B. L.; et al. Salvinorin A: a potent naturally occurring nonnitrogenous κ opioid selective agonist. *Proc. Natl. Acad. Sci. U. S. A.* **2002**, *99*, 11934−11939.

(12) Prisinzano, T. E.; Rothman, R. B. Salvinorin A analogs as probes in opioid pharmacology. *Chem. Rev.* **2008**, *108*, 1732−1743.

(13) Sherwood, A. M.; et al. Addressing structural flexibility at the A-ring on salvinorin A: discovery of a potent kappa-opioid agonist with enhanced metabolic stability. *J. Med. Chem.* **2017**, *60*, 3866−3878.

(14) Scheerer, J. R.; Lawrence, J. F.; Wang, G. C.; Evans, D. A. Asymmetric synthesis of salvinorin A, a potent κ opioid agonist. *J. Am. Chem. Soc.* **2007**, *129*, 8968−8969.

(15) Nozawa, M.; Suka, Y.; Hoshi, T.; Suzuki, T.; Hagiwara, H. Total synthesis of the hallucinogenic neoclerodane diterpenoid salvinorin A. *Org. Lett.* **2008**, *10*, 1365−1368.

(16) Hagiwara, H.; Suka, Y.; Nojima, T.; Hoshi, T.; Suzuki, T. Second-generation synthesis of salvinorin A. *Tetrahedron* **2009**, *65*, 4820−4825.

(17) Line, N. J.; Burns, A. C.; Butler, S. C.; Casbohm, J.; Forsyth, C. J. Total synthesis of (−)-salvinorin A. *Chem. - Eur. J.* **2016**, *22*, 17983−17986.

(18) White, K. L.; et al. The G protein-biased κ-opioid receptor agonist RB-64 is analgesic with a unique spectrum of activities in vivo. *J. Pharmacol. Exp. Ther.* **2015**, *352*, 98−109.

(19) Béguin, C.; et al. Synthesis and in vitro evaluation of salvinorin A analogues: effect of configuration at C(2) and substitution at C(18). *Bioorg. Med. Chem. Lett.* **2006**, *16*, 4679−4685.

(20) Munro, T. A.; et al. 8-*epi*-salvinorin B: crystal structure and affinity at the κ opioid receptor. *Beilstein J. Org. Chem.* **2007**, *3*, 1.

(21) Thompson, H. W.; Long, D. J. Stereochemical equilibrium in benzoctalones. *J. Org. Chem.* **1988**, *53*, 4201−4209.

(22) Corey, E. J.; Howe, W. J.; Orf, H. W.; Pensak, D. A.; Petersson, G. General methods of synthetic analysis. Strategic bond disconnections for bridged polycyclic structures. *J. Am. Chem. Soc.* **1975**, *97*, 6116−6124.

(23) Corey, E. J.; Long, A. K.; Rubenstein, S. D. Computer-assisted analysis in organic synthesis. *Science* **1985**, *228*, 408−418.

(24) Totrov, M.; Abagyan, R. Flexible protein-ligand docking by global energy optimization in internal coordinates. *Proteins: Struct., Funct., Genet.* **1997**, *29*, 215−220.

(25) Cunningham, C. W.; Rothman, R. B.; Prisinzano, T. E. Neuropharmacology of the naturally occurring κ-opioid hallucinogen salvinorin A. *Pharmacol Rev.* **2011**, *63*, 316−347.

(26) Bergman, Y. E.; Mulder, R.; Perlmutter, P. Total synthesis of 20-norsalvinorin A. 1. Preparation of a key intermediate. *J. Org. Chem.* **2009**, *74*, 2589−2591.

(27) Pollini, G. P.; Benetti, S.; De Risi, C.; Zanirato, V. Hagemann's ester: a timeless building block for natural product synthesis. *Tetrahedron* **2010**, *66*, 2775−2802.

(28) Kobayashi, S.; Nagayama, S.; Busujima, T. Lewis acid catalysis stable in water. Correlation between catalytic activity in water and hydrolysis constants and exchange rate constants for substitution of inner-sphere water ligands. *J. Am. Chem. Soc.* **1998**, *120*, 8287−8288.

(29) Heng, K. K.; Smith, R. A. J. Organometallic reagents in organic synthesis−V: an organocuprate conjugate addition−aldol condensation synthetic procedure for sequential formation of two carbon-carbon bonds. *Tetrahedron* **1979**, *35*, 425−435.

(30) House, H. O.; Crumrine, D. S.; Teranishi, A. Y.; Olmstead, H. D. Chemistry of carbanions. XXIII. Use of metal complexes to control the aldol condensation. *J. Am. Chem. Soc.* **1973**, *95*, 3310−3324.

(31) Davis, F. A.; Vishwakarma, L. C.; Billmers, J. G.; Finn, J. Synthesis of α-hydroxycarbonyl compounds (acyloins): direct oxidation of enolates using 2-sulfonyloxaziridines. *J. Org. Chem.* **1984**, *49*, 3241−3243.

(32) Delcamp, J. H.; Brucks, A. P.; White, M. C. A general and highly selective chelate-controlled intermolecular oxidative Heck reaction. *J. Am. Chem. Soc.* **2008**, *130*, 11270−11271.

(33) Beak, P.; Snieckus, V. Directed lithiation of aromatic tertiary amides: an evolving synthetic methodology for polysubstituted aromatics. *Acc. Chem. Res.* **1982**, *15*, 306−312.

(34) Wang, D.-H.; Engle, K. M.; Shi, B.-F.; Yu, J.-Q. Ligand-enabled reactivity and selectivity in a synthetically versatile aryl C−H olefination. *Science* **2010**, *327*, 315−319.

(35) Houpis, I. N.; et al. Carboxylate directed cross-coupling reactions in the synthesis of trisubstituted benzoic acids. *Org. Lett.* **2008**, *10*, 5601−5604.

(36) Olofsson, K.; Sahlin, H.; Larhed, M.; Hallberg, A. Regioselective palladium-catalyzed synthesis of β-arylated primary allylamine

equivalents by an efficient Pd−N coordination. *J. Org. Chem.* **2001**, *66*, 544−549.

(37) Larock, R. C.; Leuck, D. J.; Harrison, L. W. Synthesis of vinylic lactones via palladium-catalyzed coupling of vinylic halides or triflates and unsaturated carboxylic acids. *Tetrahedron Lett.* **1988**, *29*, 6399−6402.

(38) Shigehisa, H.; Aoki, T.; Yamaguchi, S.; Shimizu, N.; Hiroya, K. Hydroalkoxylation of unactivated olefins with carbon radicals and carbocation species as key intermediates. *J. Am. Chem. Soc.* **2013**, *135*, 10306−10309.

(39) Shuklov, I. A.; Dubrovina, N. V.; Börner, A. Fluorinated alcohols as solvents, cosolvents and additives in homogeneous catalysis. *Synthesis* **2007**, *2007*, 2925−2943.

(40) Morgenweck, J.; Frankowski, K. J.; Prisinzano, T. E.; Aube, J.; Bohn, L. M. Investigation of the role of βarrestin2 in kappa opioid receptor modulation in a mouse model of pruritus. *Neuropharmacology* **2015**, *99*, 600−609.

(41) Schmid, C. L.; et al. Functional selectivity of 6′-guanidinonal-trindole (6′GNTI) at κ-opioid receptors in striatal neurons. *J. Biol. Chem.* **2013**, *288*, 22387−22398.

(42) Zhou, L.; et al. Development of functionally selective, small molecule agonists at kappa opioid receptors. *J. Biol. Chem.* **2013**, *288*, 36703−36716.

(43) Lozama, A.; et al. Opioid receptor probes derived from cycloaddition of the hallucinogen natural product salvinorin A. *J. Nat. Prod.* **2011**, *74*, 718−726.

(44) Munro, T. A.; Rizzacasa, M. A.; Roth, B. L.; Toth, B. A.; Yan, F. Studies toward the pharmacophore of salvinorin A, a potent κ opioid receptor agonist. *J. Med. Chem.* **2005**, *48*, 345−348.

(45) Szymkuć, S.; et al. Computer-assisted synthetic planning: the end of the beginning. *Angew. Chem., Int. Ed.* **2016**, *55*, 5904−5937.

(46) Clemons, P. A.; et al. Small molecules of different origins have distinct distributions of structural complexity that correlate with protein-binding profiles. *Proc. Natl. Acad. Sci. U. S. A.* **2010**, *107*, 18787−18792.

(47) Dobson, C. M. Chemical space and biology. *Nature* **2004**, *432*, 824−828.

(48) Morrison, K. C.; Hergenrother, P. J. Natural products as starting points for the synthesis of complex and diverse compounds. *Nat. Prod. Rep.* **2014**, *31*, 6−14.

(49) Wender, P. A.; Verma, V. A.; Paxton, T. J.; Pillow, T. H. Function-oriented synthesis, step economy, and drug design. *Acc. Chem. Res.* **2008**, *41*, 40−49.

(50) Li, J.; Eastgate, M. D. Current complexity: a tool for assessing the complexity of organic molecules. *Org. Biomol. Chem.* **2015**, *13*, 7164−7176.

(51) Allemann, O.; Brutsch, M.; Lukesh, J. C., III; Brody, D. M.; Boger, D. L. Synthesis of a potent vinblastine: rationally designed added benign complexity. *J. Am. Chem. Soc.* **2016**, *138*, 8376−8379.

(52) After this manuscript was posted to ChemRxiv (DOI: 10.26434/chemrxiv.5318188), a paper was submitted that described a structurally simplified SalA analogue synthesized according to the route of Ref 14. Potency decreased 113-fold compared to SalA and KOR/MOR/DOR selectivity was not reported. See: Sherwood, A. M.; Williamson, S. E.; Crowley, R. S.; Abbott, L. M.; Day, V. W.; Prisinzano, T. E. *Org. Lett.* **2017**, *19*, 5414.